The Astronomical Journal, 133:2859–2865, 2007 June

THE WOLF-RAYET STARS HD 4004 AND HD 50896: TWO OF A KIND

Aaron Flores
Facultad de Ingenieria, Universidad Autonoma del Carmen, Ciudad del Carmen, Campeche, Mexico; aflores@pampano.unacar.mx

Gloria Koenigsberger
Instituto de Ciencias Fisicas, Universidad Nacional Autonoma de Mexico, Cuernavaca, Morelos 62251, Mexico; gloria@fis.unam.mx

Octavio Cardona
Instituto Nacional de Astrofisica Optica y Electronica, Puebla, Mexico; ocardona@inaoep.mx

and

Lelio de la Cruz
Facultad de Ingenieria, Universidad Autonoma del Carmen, Ciudad del Carmen, Campeche, Mexico; ldelacruz@pampano.unacar.mx
Received 2007 January 24; accepted 2007 March 13

ABSTRACT

We present the results of the analysis of 151 spectra of the Wolf-Rayet star HD 4004 (WR1) obtained in 1999 and in 2005. The line-profile variability is found to be periodic, with $P = 7.684$ days, and to have characteristics that are very similar to those of another variable WR star, HD 50896 (WR6). The similarities point toward a common physical phenomenon in both systems. Of the scenarios that can explain the observations, such as colliding winds in two stars with similar wind momenta and the ejection of streams or jets from two opposite locations on the stellar surface, the latter seems more likely due to the lack of observational evidence for a strong wind-bearing companion.

Key words: binaries: general — stars: individual (HD 4004, HD 50896) — stars: winds, outflows — stars: Wolf-Rayet

1. INTRODUCTION

Massive Wolf-Rayet (WR) stars are characterized as possessing high-velocity, radiatively driven winds, expanding with velocities in the range 1500–2500 km s^{-1}. The winds are highly unstable and believed to be permeated by internal shocks (Lucy & White 1980; Owocki & Rybicki 1991; Gayley & Owocki 1995) that are associated with density enhancements in different regions of the wind. In addition, the colliding winds in WR+O binary systems introduce an asymmetry in the wind structures, and the shock structures associated with the collision imply physical conditions that are different from the stationary wind. These phenomena are believed to be responsible for the presence of substructures superposed on the emission lines of the principal atomic transitions. Observations have shown that these substructures are variable, with the line-profile variability (LPV) timescales being (1) random (RLPV), (2) semiperiodic, and (3) periodic (PLPV) (Lépine et al. 1999). In WR binaries, PLPV arises, grows, and disappears on orbital timescales.

There are several Galactic WRs classified as single stars in which the emission lines show substructures whose pattern of variability hints at a periodic nature, but for which a period has not been determined. Periodic variability is associated with rotation or orbital motion, and determining whether the variability is periodic is the first step that is required before gaining an understanding of the physical mechanisms producing stellar wind variability. That is, in the absence of periodic modulation, binary mechanisms such as wind eclipses, wind-wind collisions, and heating effects by a companion may be discarded, constraining the mechanisms to those associated with wind instabilities or rotation effects modulated by stochastic processes. However, the search for periodicity in most of the best-studied WR single-line systems has produced inconclusive results.

For example, Morel et al. (1999b) attempted to reproduce the He II λ4686 LPV of HD 191765, assuming it to be a WR+cc binary, i.e., a relativistic compact stellar companion (cc) revolving inside the dense WR wind. However, they were able to reproduce profiles for only a portion of the assumed orbital cycle. Although quite popular, the WR+cc scenarios are faced with inconsistencies when the X-ray observations are compared with the expected X-ray luminosities from an accreting collapsed companion (Willis & Stevens 1996; Flores et al. 1999). This has resulted in a rejection of the WR+cc case. On the other hand, recent *XMM-Newton* observations of HD 50896 lead to the conclusion that this star does indeed have a stellar companion, although it is not necessarily a relativistic star (Skinner et al. 2002).

HD 4004 (WR1) is another single-line WR star for which possible periodic variability in the optical emission-line spectra on the timescale of 5–8 days has been reported (Niedzielski 2000; Morel et al. 1999a). HD 4004 was observed recently with *XMM-Newton* and showed lower X-ray luminosity than WR6 and WR110, suggesting that HD 4004 is an isolated single star rather than a binary system (Ignace et al. 2003). In this paper we present an analysis of the optical line profile variability based on a set of 151 optical spectra of this object obtained during two epochs separated by 7 yr, and we show that the variability is periodic. Thus, a binary scenario cannot be ruled out.

This paper is divided into the following sections. In § 2 we describe the observations and data reduction process, in § 3 we describe the method employed to determine the period of the variations, in § 4 we compare HD 4004 with HD 50896, and in § 5 we present a discussion and our conclusions.

2. OBSERVATIONS AND DATA REDUCTION

The observations were carried out during 1999 October 23–27 and 2005 November 19–26 with the Boller & Chivens

TABLE 1
SUMMARY OF HD 4004 OBSERVATIONAL DATA

JD (Mean) (2,450,000+)	Date	Number Collected	Time Interval (hr)	Phase (Mean)
1474.81269.....	1999 Oct 23	5	1.50	0.21
1475.81571.....	1999 Oct 24	14	3.50	0.35
1477.82635.....	1999 Oct 26	12	3.00	0.61
1478.80345.....	1999 Oct 27	11	2.50	0.73
3693.84510.....	2005 Nov 19	4	1.00	0.00
3694.70475.....	2005 Nov 20	19	4.75	0.11
3695.70636.....	2005 Nov 21	21	5.25	0.24
3696.73880.....	2005 Nov 22	17	4.25	0.38
3697.68693.....	2005 Nov 23	17	4.25	0.50
3699.79394.....	2005 Nov 25	11	2.75	0.77
3700.68476.....	2005 Nov 26	20	5.00	0.89

spectrograph of the 2.1 m Guillermo Haro telescope at the Mexican National Astronomical Observatory, in Cananea, Sonora, using a slit size of 250 μm, an 830 lines mm^{-1} grating in the second order, and a CCD Tek 1024 $\times$ 1024 detector. To avoid possible integration of the detector's internal reflections, a SCHOT BG18 blocking filter was placed at the slit entrance, thus removing light at $\lambda < 4000$ Å. For the wavelength calibration, HeAr comparison lamp spectra were obtained before each target integration. A total of 151 spectra were obtained, having reciprocal resolution of 0.31 Å pixel^{-1} and in the wavelength interval $\lambda\lambda$4455–4771. The mean Julian Dates of the observations are listed in Table 1, which also contains the date of the observation, the number of spectra collected, and the corresponding time interval during which these spectra were obtained.

Data reduction was performed using standard procedures from the Image Reduction and Analysis Facility (IRAF) package,[1] which included bias subtraction, flat-field correction, and cosmic-ray deletion. The spectra were normalized to the continuum level after interpolating a third-order Legendre polynomial function to line-free spectral regions.

3. LINE-PROFILE VARIATIONS

Figure 1 (*top panels*) illustrates the individual spectra of 1999, stacked with small vertical offsets with time increasing upward. The three emission lines that are plotted are He II λ4540, N V $\lambda\lambda$4603–4621, and He II λ4686. Larger vertical shifts separate data of different nights. The most prominent variations are visible in He II λ4686, with timescales of $\sim$1 day. On the first night of the observations, it has a relatively flat-looking top, with little or no change visible throughout the 1.5 hr of observations. During night 2, there is a central peak that persists during the 3.5 hr of observations. The next night was cloudy, and only one very poor quality spectrum was acquired, which also shows one peak. By the next night, the central peak appears to have split into two components whose separation increases throughout the night, a trend that continues into the next night. Both He II lines display the same trend. The average separation of the peaks practically doubles from one night to the next, going from $\sim$870 km s^{-1} on 1999 October 26 to $\sim$1300 km s^{-1} on 1999 October 27.

Figure 2 illustrates the data obtained in 2005. The individual line profiles for the seven nights are plotted as in Figure 1, showing

[1] IRAF is distributed by the National Optical Astronomy Observatory, which is operated by the Association of Universities for Research in Astronomy, Inc., under cooperative agreement with the National Science Foundation.

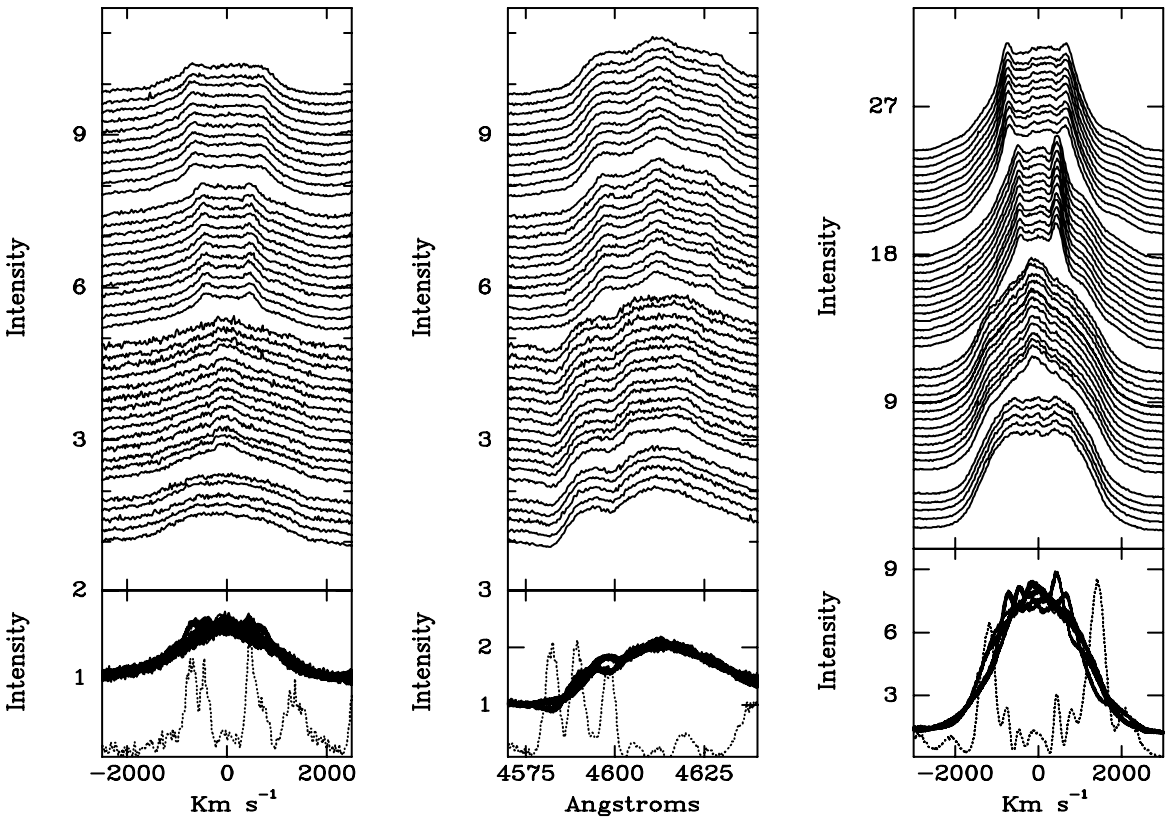

FIG. 1.—Line-profile variations of He II λ4540 (*left*), N V $\lambda\lambda$4603–4621 (*middle*), and He II λ4686 (*right*) in HD 4004 data obtained in 1999. The top panels contain individual spectra, displaced vertically in order of increasing time, with larger separations to indicate different nights of observation. The bottom panels display the superposition of all spectra without vertical shifts, and the corresponding TVS$_\lambda$, which indicates wavelengths where the line profile is most variable.

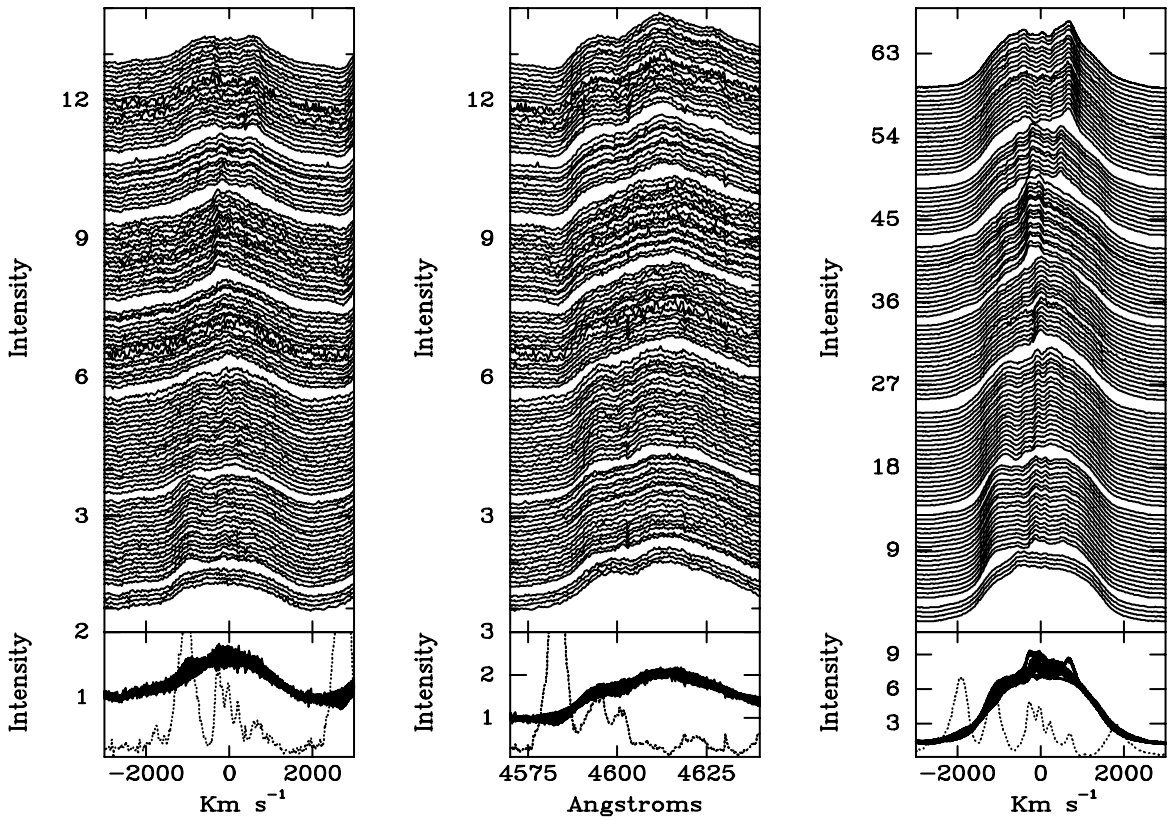

FIG. 2.—Same as Fig. 1, but for the data of 2005 (epoch II).

a similar (but not identical) trend from a flat-looking top to a central peak to a double peak, as in the 1999 data. Although the intensity of the peaks in 2005 is somewhat different from that in 1999, the variability phenomenon can be described in general terms as one in which two narrow emission features move from side to side on the broad underlying profile. When they coincide, the result is a single, centrally located peak. Otherwise, the peaks are separated and less intense than the single peak.

In order to quantify the variability, we calculate the time-variance spectrum (TVS), which is especially useful in determining the wavelength location of variability. Following Fullerton et al. (1996) and Henrichs et al. (1994), the TVS is given by

$$(\mathrm{TVS})_\lambda = \frac{1}{N-1}\sum_{i=1}^{N}\left[\frac{F_i(\lambda)-\bar{F}(\lambda)}{\sigma_i(\lambda)}\right]^2, \qquad (1)$$

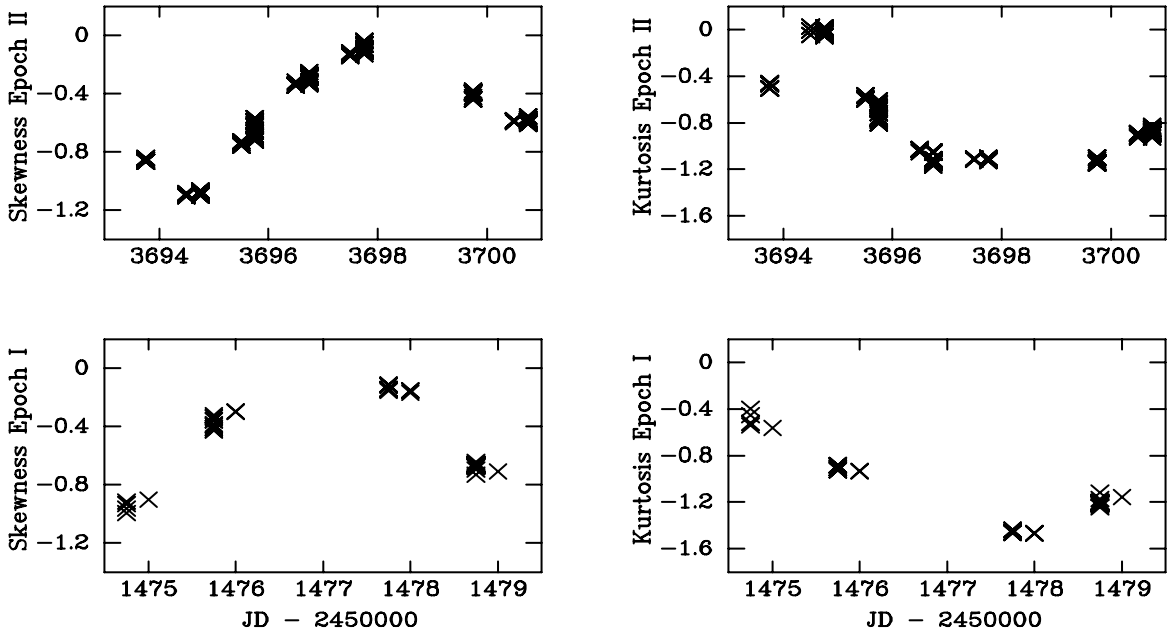

FIG. 3.—Skewness and kurtosis of the He II λ4686 profile vs. Julian Date, for the data obtained during the two epochs. A clear modulation in both data sets is present.

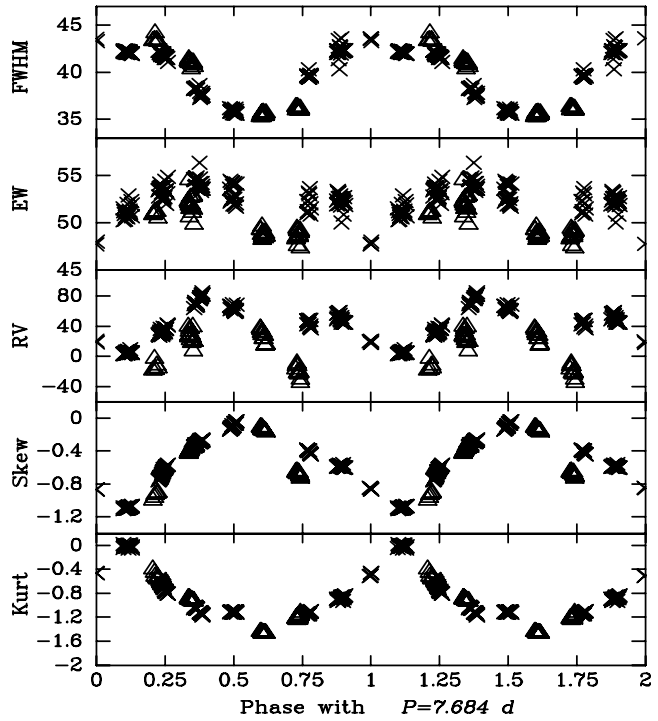

FIG. 4.—Kurtosis, skewness, RV, EW, and FWHM of He II λ4686 folded with the $P = 7.684$ day period. Triangles represent data obtained in 1999 (epoch I), while crosses represent the data of 2005 (epoch II). FWHM and EW are given in angstroms, with RV in kilometers per second.

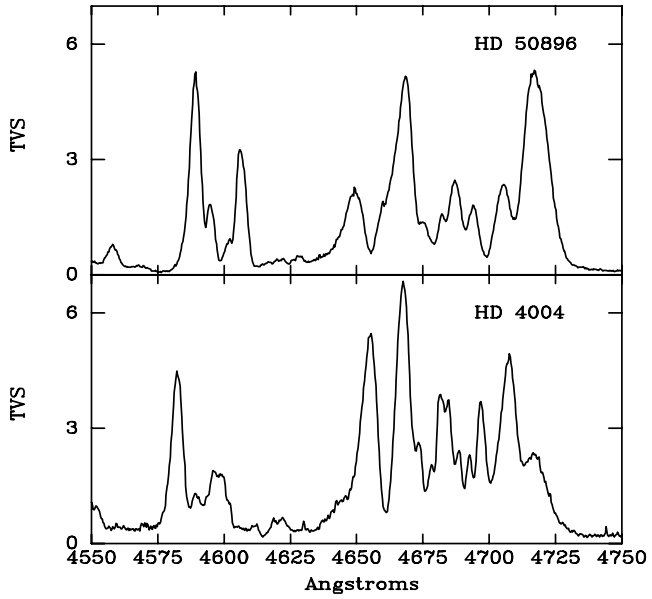

FIG. 5.—$(\mathrm{TVS})_\lambda$ plots that locate the wavelength position where the emission lines are most variable, for HD 50896 (*top*) and HD 4004 (*bottom*). The variability in both stars is very similar.

where $\bar{F}_w(\lambda)$ is the constructed weighted mean spectrum, $F_i(\lambda)$ are the individual spectra, and $\sigma_i(\lambda) = F_i(\lambda)/\mathrm{S/N}$ of the individual pixels of the spectra.

The temporal sigma spectrum $(\mathrm{TSS}) = (\mathrm{TVS})^{1/2}$ represents approximately $(\sigma_{\mathrm{obs}}/\bar{\sigma})$. This is the standard deviation of the variations of the individual spectra with respect to the average spectrum. If no significant variations are present, the value will be close to unity. The bottom panels in Figures 1 and 2 display all spectra superposed without vertical shifts, together with the $(\mathrm{TVS})_\lambda$. Although the "dancing" peaks on the top of the lines are the most obvious to the eye, the strongest variability actually occurs on the blue wings of the lines.

4. PERIODICITY DETERMINATION

Two additional quantities that provide information on the shape of the line profile are the third and fourth statistical moments, otherwise known as the skewness and the kurtosis, respectively (Press et al. 2002). The skewness indicates the degree of asymmetry of the feature, and the kurtosis describes whether the profile is highly peaked or has a flat top. These quantities were obtained for the upper portion of the He II λ4686 line profile, specifically for the portion of the profile that lies above $I = 3$, where $I = 1$ corresponds to the continuum level. In Figure 3 we plot the statistical moments as a function of Julian Date, illustrating the results for the 1999 data and the 2005 data separately. The curves clearly indicate a periodic trend, consistent with the findings of Morel et al. (1999a) and Niedzielski (2000), who reported systematic behavior of their data on timescales of 5–8 days.

Applying the Scargle method (Scargle 1982) to each epoch separately yields possible periods of $P = 6.658$ and 8.258 days in both data sets. However, neither of these periods produces a modulated curve when the data of both epochs are combined. However, if the period search is conducted on the combined data set, three periods emerge: $P = 6.658$, 7.684, and 8.258 days. Folding the data with $P = 7.684$ days produces a smooth modulated curve, which is illustrated in Figure 4. The significance of this result lies in the fact that two data sets that were obtained during two epochs separated by 7 yr present a periodic modulation with $P = 7.684$ days. The long-term presence of a single period suggests that the underlying mechanism for the variability is either stellar rotation or interaction effects in a binary system.

Additional diagnostics of spectral variability, such as the equivalent width (EW), full width at half-maximum intensity (FWHM), and radial velocity (RV) are also modulated with the same period. The FWHM corresponds to that of a Gaussian fit to the line profile of He II λ4686. The other quantities were measured on the top portion of the He II λ4686 emission line only. The EW measurement corresponds to the area under the line profile and above $I = 3$, where $I = 1$ corresponds to the continuum level. Similarly, the RV was obtained by dividing in half the area in the line profile above $I = 3$. In Figure 4 these quantities are plotted as a function of phase computed with $P = 7.684$ days. Phase $\phi = 0$ corresponds to $T_0 = \mathrm{JD}\ 2{,}453{,}693.845$. At this phase there is a minimum in the EW of the He II λ4686 line, and the FWHM is maximum. The skewness, kurtosis, and FWHM show the smoothest modulation. The RV curve has a systematic shift between the values of both epochs, particularly evident at $\phi = 0.75$, at which time the difference is $\sim$50 km s^{-1}. The origin of this systematic difference is not understood, and thus it is not clear whether we can associate the curve with orbital motion, even assuming that the system is a binary.

5. COMPARISON WITH HD 50896

HD 50896 has long been known to exhibit periodic line-profile variability with $P = 3.76$ days (Firmani et al. 1980; Georgiev et al. 1999; Flores 2000), although the coherence of some of the variations persists only for timescales of $\sim$2 weeks (Moffat 1983). The line-profile variability in HD 4004 is qualitatively very similar to that observed in HD 50896. Using the 151 spectra of HD 4004 and the 160 spectra that we have of HD 50896 (Flores 2000), it is now possible to do a quantitative comparison between these two stars. In Figure 5 we plot the TVS in the wavelength

TABLE 2
WAVELENGTH VELOCITY OF COINCIDENT TVS PEAKS OF HD 4004 AND HD 50896

HD 4004 (WR1)			HD 50896 (WR6)		
Wavelength (λ)	ID	Velocity (km s^{-1})	Wavelength (λ)	ID	Velocity (km s^{-1})
4582.....	N v 4603	−1350	4589.....	N v 4603	−904
4597.....	N v 4621	−1545	4606.....	N v 4621	−957
4654.....	He II(?)	−1998	4650.....	He II(?)	−2347
4667.....	He II 4686	−1161	4667.....	He II	−1155
4707.....	He II	+1381	4704.....	He II	+1236
4717.....	He II	+1972	4717.....	He II	+2431

range $\lambda\lambda$4550–4750 for both stars, and in Table 2 the location of the strongest TVS peaks is listed. It is important to note that an adequate comparison of the TVS for the two stars is possible because of the complete phase coverage in the two data sets and the long time span over which the data were collected. Limited data sets yield TVS plots that are either biased by poor phase coverage or present predominantly epoch-to-epoch variability, rather than represent the periodic variability. Our data sets have complete phase coverage and were obtained over many years of observations, avoiding both of these problems.

The wavelength listed in Table 2 corresponds to that of the atomic species with which the feature is identified, and the velocity is measured with respect to this wavelength. There is a large degree of similarity in the TVS of the two stars. Noteworthy is the fact that the strongest variability in both stars occurs on the wings of the lines and, in the case of N v, the strong TVS peaks can be clearly associated with the P Cygni–like absorption components. In HD 4004 the strongest variability of N v P Cygni absorptions occurs at -1450 ± 100 km s^{-1}, while in HD 5980 it is at -930 ± 25 km s^{-1}. Because P Cygni absorption components are formed only in the expanding gas that is projected on a background continuum source, the strong variability in these features indicates that the characteristics of the outflowing wind

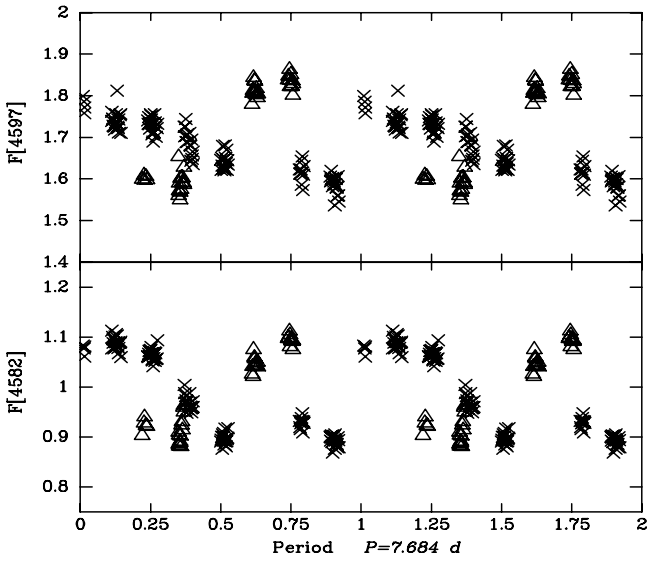

FIG. 6.—Integrated intensity within the wavelength intervals corresponding to the N v doublet, where (TVS)$_\lambda$ maxima appear. These wavelength intervals coincide with the P Cygni–like troughs. The trend for two maxima (at $\phi = 0.20$ and 0.75) and two minima (at $\phi = 0.50$ and 0.90) is similar to that which is observed for HD 50896. Triangles represent data obtained during epoch I, while crosses represent the data of epoch II.

are not constant with time. In HD 50896 the variability that is most stable over long timescales is that of the N v P Cygni absorption components (Georgiev et al. 1999; Flores 2000). Their strength varies systematically with the 3.76 day period. This implies that the modulation of the outflow velocity in the stellar wind is periodic, thus eliminating stochastic processes as the mechanism inducing the variability.

In order to determine how the P Cygni absorption troughs vary as a function of phase in HD 4004, we integrated their intensity in the wavelength windows $\lambda\lambda$4580–4584 and $\lambda\lambda$4595–4600. The phase dependence of these quantities is illustrated in Figure 6, showing that there appear to be two maxima (at $\phi = 0.20$ and 0.75) and minima (at $\phi = 0.50$ and 0.90) per cycle. This is the same behavior that Georgiev et al. (1999) found in HD 50896.

We are thus led to conclude that the phenomenon that causes the emission-line profile variability in HD 4004 has the same origin as that which is present in HD 50896, and that both stars provide a testing ground for understanding the underlying mechanism responsible for their variability.

6. DISCUSSION AND CONCLUSIONS

The superposed narrow peaks on the He II line profiles in HD 4004 suggest the presence of two oppositely directed outflows from the star, whose projected velocity changes due to rotation in the system from which these outflows emerge. This effect can be quantified by separating the superposed peaks from the underlying, broader emission component. We chose the spectrum obtained on 2005 November 19 as the template for the underlying emission, because in this spectrum the emission lines are weak compared to the rest of the data, and the superposed peaks are least prominent. This spectrum, which was also chosen to define $\phi = 0$, was subtracted from all of the other observations from both epochs. The result is illustrated in Figure 7 (*top panels*), where gray-scale representations of the residual emission are presented. The data are stacked from the bottom to the top in order of increasing phase, computed with $P = 7.684$ days. The bottom panels contain the residuals for 10 equally spaced phase bins. Both He II lines present the same trend, which consists of opposite motion within the velocity interval ± 1000 km s^{-1} of two residual emission peaks. This motion is confirmed by plotting the centroid of the sharp peaks as a function of phase, as illustrated in Figure 8 for He II λ4686, where we use the data of the same 10 phase bins plotted in the bottom panels of Figure 7. The data plotted in the two middle panels (with ordinate in the range ± 1500 km s^{-1}) describe two sinusoidal curves that intersect at orbital phase $\sim$0.5. When they intersect, there is only one centrally placed, superposed peak on He II λ4686.

Although not evident on the gray-scale plots of Figure 7, there is a second set of residual emission lines located at ~ -2500 and

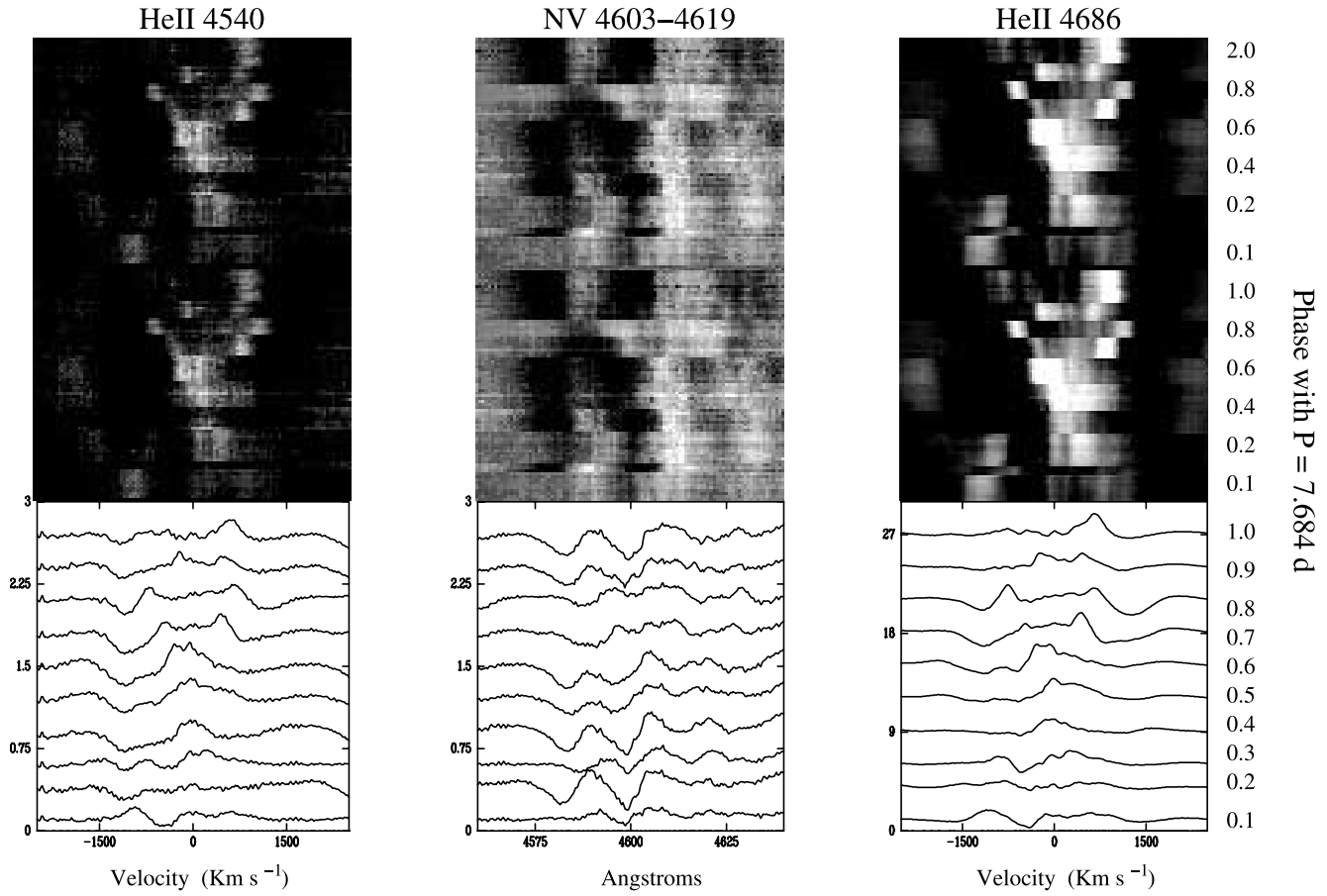

FIG. 7.—*Top panels*: Gray-scale panels showing the variations of the emission residuals that result from subtracting the spectrum of 2005 November 19 from the other spectra. Phase calculated with $P = 7.684$ days increases from the bottom to the top. *Bottom panels*: Residual emission for spectra in 10 phase bins.

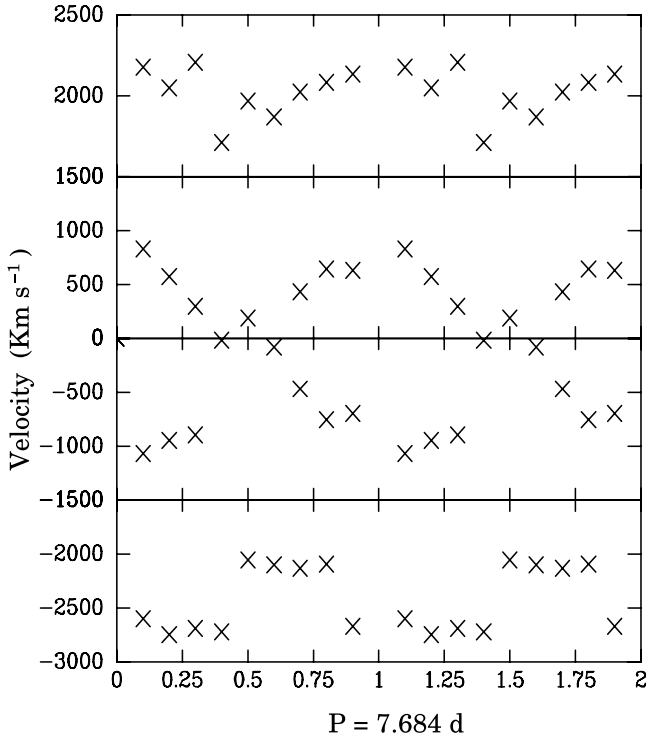

FIG. 8.—Modulation of the projected radial velocity variations of the He II λ4686 residual emission subpeaks.

$\sim$+2000 km s^{-1}, which also move in antiphase with each other. Their RV variations are plotted in Figure 8.

In summary, we find that the line-profile variability of the Wolf-Rayet star HD 4004 is periodic, with $P = 7.684$ days. The variability is present in the He II emission-line wings, on superposed narrow emission features that "dance" back and forth on the underlying broader wind emission, and in the P Cygni absorption components of N V, which become weaker at specific phases. The TVS of HD 4004 is very similar to that of the well-studied WR star HD 50896, as are the line-profile shapes and variability trends of equivalent width. The main difference between HD 4004 and HD 50896 is the periodicity timescale, which in the latter is $P = 3.76$ days. Thus, we conclude that the same mechanism inducing the variability is present in both stars.

HD 50896 was originally suspected of being a binary system harboring a collapsed companion (Koenigsberger 1978; Firmani et al. 1980). However, the X-ray luminosity has been shown to be too low to be associated with accretion onto a neutron star or black hole, although a binary mechanism is still the preferred scenario (Skinner et al. 2002). Within a binary scenario, there are several mechanisms that may produce line-profile variability, but among the standard ones, only wind-wind collisions (WWCs) can lead to the appearance of superposed narrow emission features at velocities of 1000 km s^{-1} or more. If the stellar winds have similar momenta and mechanical energies, the WWC region could produce the large-amplitude, antiphase motion of the superposed emission peaks. This scenario, however, requires the alleged companion to possess a very strong wind, and thus it should be massive and luminous enough to be detected. This is the case,

for example, in the WN5+O6 binary system V444 Cygni, for which Flores et al. (2001) found that the narrow emission that is superposed on the broad wind feature could originate in the WWC zone. Thus, in the case of HD 4004, it is difficult to understand how one might be dealing with a wind-wind colliding WR binary without evidence of a massive and luminous companion.

A second scenario, which was proposed by Matthews et al. (1992) to explain the line-profile variability in HD 50896, consists of the presence of two oppositely directed outflows from the stellar surface, which, due to the rotation of the star, produce the "back-and-forth" motion of the superposed peaks. This scenario does not necessarily require the star to be a binary. Under certain conditions, prolate mass loss due to gravity darkening (e.g., Cranmer & Owocki 1995) may produce a nonspherically symmetric wind structure. The effect on the shape and variability of the emission lines may simulate that of two counterdirected mass streams.

On the other hand, Moreno et al. (2005) and Toledano et al. (2006) have suggested that the shear energy dissipation due to tidal forces in asynchronous binary systems may lead to activity that includes enhanced mass ejection at specific locations on the stellar surface. This might provide another potential physical mechanism in the Matthews et al. scenario, but requires the system to be a binary.

Further progress in constraining the model to explain HD 4004 and HD 50896 requires the calculation of line profiles under the assumption of two (or more) regions on the stellar surface with enhanced mass loss in order to compare with the observational line profiles.

We appreciate the allocation of observing time at Guillermo Haro observatory. We thank Ken Gayley for reviewing the manuscript and providing valuable comments. This work was supported by UNACAR grant 05-DIP-2004 and UNAM/DGAPA/PAPIIT grant IN 119205.

REFERENCES

Cranmer, S. R., & Owocki, S. P. 1995, ApJ, 440, 308
Firmani, C., Koenigsberger, G., Bisiacchi, G. F., Moffat, A. F. J., & Isserstedt, J. 1980, ApJ, 239, 607
Flores, A. 2000, Ph.D. thesis, INAOE, Mexico
Flores, A., Auer, L. H., Koenigsberger, G., & Cardona, O. 2001, ApJ, 563, 341
Flores, A., Cardona, O., & Koenigsberger, G. 1999, in IAU Symp. 193, Wolf-Rayet Phenomena in Massive Stars and Starburst Galaxies, ed. K. A. van der Hucht, G. Koenigsberger, & P. R. J. Eenens (San Francisco: ASP), 65
Fullerton, A. W., Gies, D. R., & Bolton, C. T. 1996, ApJS, 103, 475
Gayley, K. G., & Owocki, S. P. 1995, ApJ, 446, 801
Georgiev, L. N., Koenigsberger, G., Ivanov, M. M., St.-Louis, N., & Cardona, O. 1999, A&A, 347, 583
Henrichs, H. F., Kaper, L., & Nichols, J. S. 1994, A&A, 285, 565
Ignace, R., Oskinova, L. M., & Brown, J. C. 2003, A&A, 408, 353
Koenigsberger, G. 1978, Tesis Profesional de Licenciatura, Facultad de Ciencias, UNAM
Lépine, S., Shara, M. M., Livio, M., & Zurek, D. 1999, ApJ, 522, L121
Lucy, I. B., & White, R. L. 1980, ApJ, 241, 300
Matthews, J. M., St.-Louis, N., Moffat, A. F. J., Drissen, L., Koenigsbevger, G., Cardona, O., & Niemela, V. S. 1992, in ASP Conf. Ser. 22, Nonisotropic and Variable Outflows from Stars, ed. L. Drissen, C. Leitherer, & A. Nota (San Francisco: ASP), 130
Moffat, A. F. J. 1983, in Wolf-Rayet Stars: Progenitors of Supernovae?, ed. M.-C. Lortet & A. Pitault (Paris: Obs. Paris), III-13
Morel, T., Georgiev, L. N., Grosdidier, Y., St-Louis, N., Eversberg, T., & Hill, G. M. 1999a, A&A, 349, 457
Morel, T., et al. 1999b, ApJ, 518, 428
Moreno, E., Koenigsberger, G., & Toledano, O. 2005, A&A, 437, 641
Niedzielski, A. 2000, A&A, 362, 289
Owocki, S. P., & Rybicki, G. B. 1991, ApJ, 368, 261
Press, W. H., et al. 2002, Numerical Recipes in C (Cambridge: Cambridge Univ. Press)
Scargle, J. D. 1982, ApJ, 263, 835
Skinner, S. L., Szhekov, S. A., Güdel, M., & Schmutz, W. 2002, ApJ, 579, 764
Toledano, O., Moreno, E., Koenigsberger, G., Detmers, R., & Langer, N. 2007, A&A, 461, 1057
Willis, A. J., & Stevens, I. R. 1996, A&A, 310, 577